

Star-Shaped Polymer PFStODO by Atom Transfer Radical Polymerization: Its Synthesis, Characterization, and Fluorescence Property

Pei-Yang Gu,¹ Cai-Jian Lu,¹ Qing-Feng Xu,¹ Gao-Jie Ye,¹ Wei-Qiang Chen,² Xuan-Ming Duan,² Li-Hua Wang,¹ Jian-Mei Lu¹

¹Key Laboratory of Organic Synthesis of Jiangsu Province, College of Chemistry, Chemical Engineering and Materials Science, Soochow University, Suzhou, Jiangsu 215123, China

²Laboratory of Organic NanoPhotonics and Key Laboratory of Functional Crystals and Laser Technology, Technical Institute of Physics and Chemistry, Chinese Academy of Sciences, No.2, Beiyitiao, Zhongguancun Road, Haidian District, Beijing 100190, China

Correspondence to: J.-M. Lu (E-mail: lujm@suda.edu.cn) or Q.-F. Xu (E-mail: xuqingfeng@suda.edu.cn)

Received 14 June 2011; accepted 8 October 2011; published online 7 November 2011

DOI: 10.1002/pola.25055

ABSTRACT: A novel monomer bearing with pyrazoline chromophore, 3-(4-fluorophenyl)-1-phenyl-5-(4-(4-vinylbenzyloxy)-phenyl-4,5-dihydro-1H-pyrazole (FStODO), was synthesized, and its atom transfer radical polymerization initiated by a tetrafunctional initiator, pentaerythritol tetrakis(2-bromoisobutyrate) (4Bri-Bu), was studied in detail and characterized by ¹H NMR, GPC, and TG-DSC. The solution, film luminescence of monomer, and its polymer were studied in detail. Compared with that of monomer, both luminescence emission intensity and quantum yield of star-shaped polymer PFStODO in DMF solution are decreased. However, the two-photon absorption (TPA) spectra in DMF solution measured by a femtosecond laser show an

entirely different result that the maxima TPA cross-section value of polymer reaches to 203 GM, better than that of the monomer itself (13 GM). More interestingly, the film of polymer shows surprisingly white emission ranging from 400 to 700 nm assigned to the excimer formation. We attribute this formation of excimers to the ordered chromophore aggregates in film, which is further verified by X-ray diffraction. © 2011 Wiley Periodicals, Inc. *J Polym Sci Part A: Polym Chem* 50: 480–487, 2012

KEYWORDS: atom transfer radical polymerization (ATRP); films; fluorescence; functionalization of polymers; pyrazoline; star polymers; white color emission

INTRODUCTION Pyrazoline and its derivatives, one of the most popular heterocyclic organic luminescent materials, have attracted growing attention due to their potential applications including fluorescence probes,¹ organic light-emitting diodes,² organic one-dimensional nanomaterials,³ nonlinear optical materials,⁴ biological activities,^{5–8} and so on.^{9–12} For example, Yao and coworkers³ have proved 1,3,5-triphenyl-2-pyrazoline is not only a good blue light emitter but also an electron donor compound. Its single crystalline nanowires can emit pure blue light, and the emission colors were tunable by doping rubene, but in the amorphous film, such phenomenon cannot be observed. Moreover, the easy crystallization and phase separation of pyrazoline-based small molecules would affect the long-term stability and would limit the applications in large area fabrications. To solve the problem, preparation of polymers bearing with pyrazoline segment in its side chain or main chain could be an effective method.^{13–17} Two methods are applied in the preparation of pyrazoline-containing polymers: one is pyrazoline conjugated polymer^{13–17} and the other is flexible polymer bearing with pyrazoline chromophore.¹⁸ We

are focusing on later, especially the flexible star-shaped polymers, the simplest type of branched polymer.

Star-shaped polymers are studied especially from the viewpoints of their potential applications for film and fabricate device with much lower synthetic cost and better long-term stability.¹⁹ With recent progress in living radical polymerization, the synthesis of star polymers has received enough attention, and various functional monomers are available for the star polymer formation, which are difficult to reach in living ionic polymerization routes, such as atom transfer radical polymerization (ATRP), reversible addition–fragmentation chain transfer polymerization, and nitroxide-mediated polymerization.¹⁹ Among them, ATRP is a more attainable method because of facile multifunctional initiators, relatively moderate polymerization condition, and low polydispersity indices. Furthermore, ATRP is an established technique in our group for polymerization of functional monomers.^{20,21} For instance, we utilize an orange emission monomer 4-(2-benzothiazole-2-yl-vinyl)-phenyl methacrylate and a blue emission initiator to obtain a white emission polymer by ATRP method.

Additional Supporting Information may be found in the online version of this article.

© 2011 Wiley Periodicals, Inc.

In this article, by utilizing ATRP, we reported a star-shaped polymer with pyrazoline chromophore at side chain. A novel blue emissive monomer with pyrazoline segment, 3-(4-fluorophenyl)-1-phenyl-5-(4-(4-vinylbenzyloxy)phenyl)-4,5-dihydro-1H-pyrazole (FStODO), was designed and synthesized. Its ATRP initiated by a tetrafunctional initiator, pentaerythritol tetrakis(2-bromoisobutyrate) (4Bri-Bu), was studied in detail and characterized by ^1H NMR, Gel Permeation Chromatography (GPC), and Thermogravimetry - Differential Scanning Calorimetry (TG-DSC) measurement. The luminescent property of monomer and its star-shaped polymer were studied in detail. They show similar emission wavelength with $\lambda_{\text{max}} = 465$ nm and the fluorescence quantum yields (Φ) were 73% (monomer) and 40% (polymer). Although, there is obvious emission intensity decreasing in one-photon fluorescence (OPF), the cross sections of two-photon absorption (TPA) of star-shaped polymer are much higher than that of monomer. More interestingly, the films of polymers prepared whether by spin coating or dispensing on quartz are surprisingly white emissive within whole visible-light region. It could be assigned to the formation of excimer, which is caused by ordered aggregate of chromophores in the side chain.

EXPERIMENTAL

CuCl (Sinopharm Chemical Reagent, 98.5%) was purified in hydrochloric acid, washed with methanol, and dried under vacuum to afford a white powder. Cyclohexanone and N,N,N',N'',N'' -pentamethyldiethylenetriamine (PMDETA) were distilled under vacuum. 4-Vinylbenzyl chloride (TCI, 90%) was obtained by column chromatography (aluminum oxide, neutral). 2-Bromo-2-methylpropionyl bromide and 4'-fluoroacetophenone (Alfa Aesar, 99%), tetramethylolmethane, 4-hydroxybenzaldehyde, phenylhydrazine (Sinopharm Chemical Reagent). All other reagents and solvents were analytically pure and were used as received without further purification.

Synthesis of Initiator

4Bri-Bu was synthesized as described in the corresponding references.²² ^1H NMR (DMSO- d_6 , 400 MHz), δ (ppm): 4.28 (s, 8H), 1.91 (s, 24H).

Preparation of Monomer and Polymers

Monomer is prepared in three steps (Supporting Information) and characterized by ^1H NMR.

4-4(Vinylbenzyloxy)benzaldehyde (BzDD)

^1H NMR (DMSO- d_6 , 400 MHz), δ (ppm): 9.8 (s, 1H), 7.87 (d, 2H), 7.51 (d, 2H), 7.44 (d, 2H), 7.20 (d, 2H), 6.76 (m, 1H), 5.85 (d, 1H), 5.28 (d, 1H), 5.23 (s, 2H).

1-(4-Fluorophenyl)-3-(4-(4-vinylbenzyloxy)phenyl)prop-2-en-1-one (FPhPP)

^1H NMR (CDCl₃, 400 MHz), δ (ppm): 8.06 (t, 2H), 7.80 (d, 1H), 7.61 (d, 2H), 7.42 (m, 5H), 7.18 (t, 2H), 7.01 (d, 2H), 6.73 (q, 1H), 5.78 (d, 1H), 5.28 (d, 1H), 5.11 (s, 2H).

3-(4-Fluorophenyl)-1-phenyl-5-(4-(4-vinylbenzyloxy)phenyl)-4,5-dihydro-1H-pyrazole (FStODO)

^1H NMR (DMSO- d_6 , 400 MHz), δ (ppm): 7.79 (t, 2H), 7.46 (d, 2H), 7.38 (d, 2H), 7.19 (m, 6H), 7.97 (t, 4H), 6.69 (t, 2H),

5.81 (d, 1H), 5.40 (q, 1H), 5.24 (d, 1H), 5.02 (s, 2H), 3.85 (q, 1H), 3.06 (q, 1H).

ATRP Polymerization of FStODO

FStODO was initiated by tetrafunctional initiator 4Bri-Bu as the following procedure: FStODO, initiator, CuCl, and PMDETA were dissolved in cyclohexanone, and the mixture was placed into a two-neck round-bottomed flask. The flask was sealed and cycled between vacuum and Ar (g) for three times. Samples were taken out by a syringe at different time intervals and diluted with tetrahydrofuran (THF). The diluted solution was passed through an alumina column to remove the copper catalyst, and the filtrate was precipitated by addition of methanol. The precipitation was filtrated and dried under vacuum.

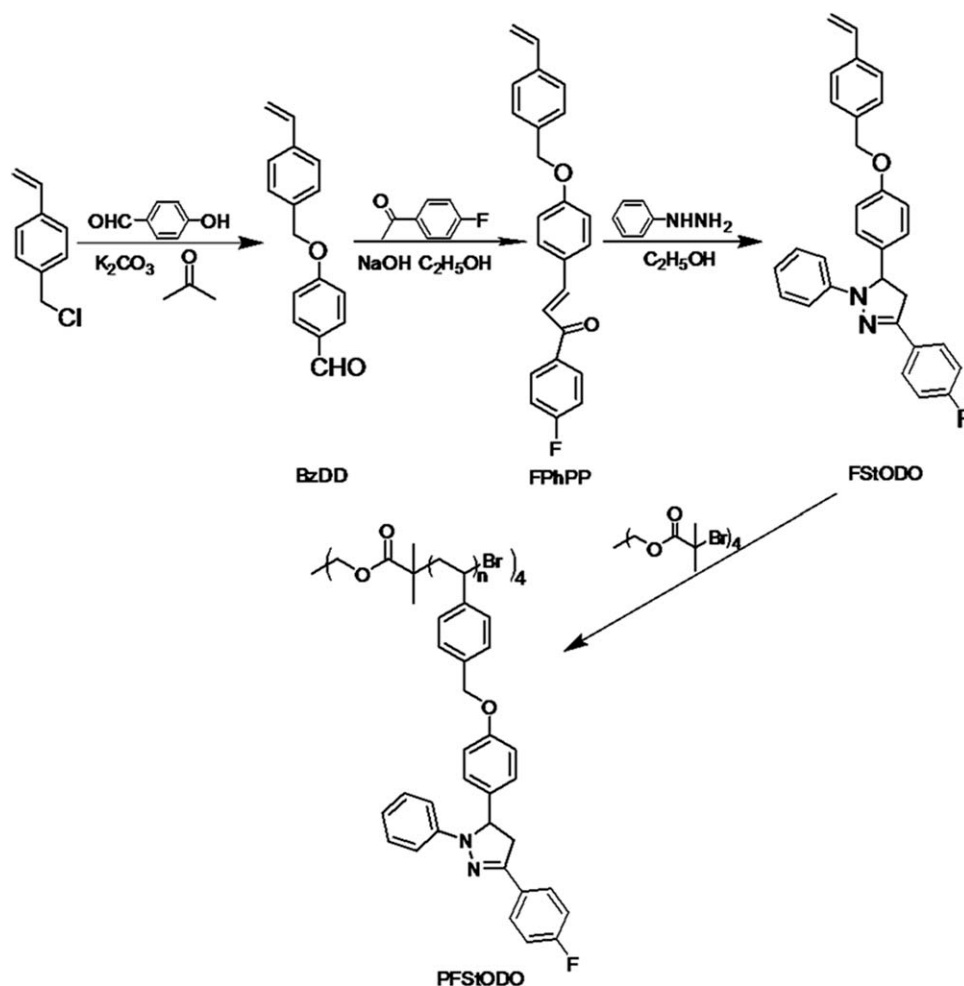
Fabrication of Films

The 1,2-dichloroethane or THF solution of PFStODO (0.5 mmol/L) was spin-coated (2000 r s⁻¹, 40 s) (or dipped) onto quartz surface and evaporated under atmosphere at room temperature. All obtained films are transparent.

Measurements

Conversions for monomer were determined by gravimetry. ^1H NMR spectra were measured using INOVA 400 MHz NMR spectrometer, CDCl₃ or DMSO- d_6 as solvent, and tetramethylsilane as the internal standard at ambient temperature. The purity was determined with a Waters515 HPLC apparatus: a mixture of methanol and water (methanol:water = 80:20, v/v) was used as the eluent at a flow rate of 0.8 mL/min at 30 °C with a C18 column and with a Waters 996 detector. Molecular weights and the polydispersity relative to PSt were measured using Waters1515 GPC with THF as a mobile phase at a flow rate of 1 mL/min and with column temperature of 30 °C. UV-vis absorption spectra of the polymers and initiator in DMF solutions were determined on a Shimadzu RF540 spectrophotometer. Room temperature emission and excitation spectra were carried out using Edinburgh-920 fluorescence spectra photometer, and fluorescence lifetimes were measured with a Fluorolog[®]-3 spectrometer. Wide-angle X-ray diffraction (XRD) patterns were taken on an X' Pert-Pro MPD X-ray diffractometer.

Two-photon excited fluorescence (TPEF) spectra were recorded on a SD2000 spectrometer (Ocean Optical) with excitation using a femtosecond laser (Tsunami, Spectra-Physics) with 100-fs pulse width and 82 MHz repetition rate. TPA cross sections were determined by the TPEF method.²³ It is assumed that the quantum efficiencies after two-photon excitation are the same as those after one-photon excitation. The TPA cross sections are obtained by calibration against fluorescein with known $\Phi\delta$ value in aqueous NaOH solution (pH = 11) at concentrations of 1.0×10^{-4} M. The samples were dissolved in solvents at concentrations of about 1.0×10^{-4} M. The error of TPEF measurement is about 15%. To ensure that the measured signals were solely due to TPA, the dependence of TPEF on the incident intensity was verified in each case to be quadratic. Then, the TPA



SCHEME 1 Synthetic scheme of FStODO and PFSStODO.

cross sections δ were calculated on the basis of the following expression:

$$\delta_s = \delta_r \frac{C_r n_r F_s \Phi_r}{C_s n_s F_r \Phi_s} \quad (1)$$

where δ is TPA cross section, C and n are the concentration and refractive index of the sample solution, respectively, and F is the integrated area under the TPEF spectrum.

RESULTS AND DISCUSSION

Characterization of Polymerization

Preparation of monomer and polymer is presented in Scheme 1. The monomer FStODO was prepared by the reaction of α,β -unsaturated ketones and hydrazines using ethanol as solvent. It is easy to dissolve in common organic solvents such as ketone, THF, and DMF. The ATRP of FStODO was performed using 4Bri-Bu as a tetrafunctional initiator in cyclohexanone at 100 °C with $[\text{FStODO}]_0:[4\text{Bri-Bu}]_0:[\text{CuCl}]_0:[\text{PMDETA}]_0 = 70:1:1:2$, $[\text{FStODO}]_0 = 0.4454 \text{ M}$, and the results are shown in Figures 1 and 2. According to Figure 1, the linearity of the semilogarithmic plot of $\ln([M]_0/[M])$ versus the polymerization time indicates that the polymerization is

first-order with respect to monomer. The number average molecular weights (M_n) increases linearly with the conversion and the polydispersity indices (PDIs) keep relatively narrow in all cases ($M_w/M_n = 1.20\text{--}1.33$), indicating the

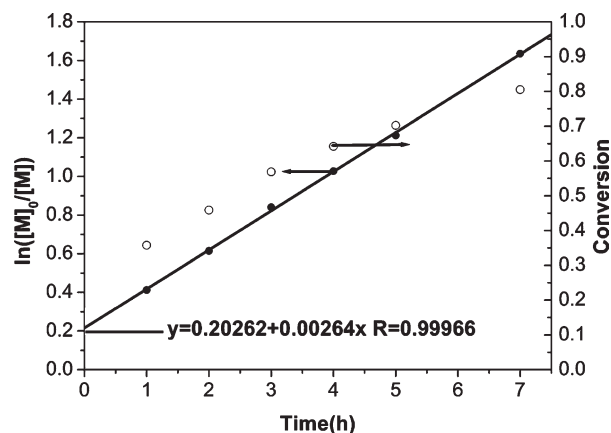


FIGURE 1 Kinetic plot for the ATRP of FStODO initiated by 4Bri-Bu in cyclohexanone solution ($[\text{FStODO}]_0:[4\text{Bri-Bu}]_0:[\text{CuCl}]_0:[\text{PMDETA}]_0 = 70:1:1:2$, $[\text{FStODO}]_0 = 0.4454 \text{ M}$, 100 °C).

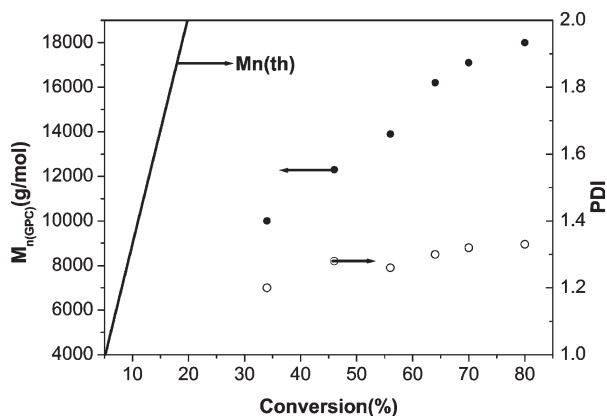


FIGURE 2 Dependence of $M_{n(\text{GPC})}$ (g/mol) and PDI with conversion for the polymerization of FStODO initiated by 4Bri-Bu in cyclohexanone solution ($[\text{FStODO}]_0$: $[\text{4Bri-Bu}]_0$: $[\text{CuCl}]_0$: $[\text{PMDETA}]_0 = 70$: 1 : 1 : 2 , $[\text{FStODO}]_0 = 0.4454 \text{ M}$, 100°C).

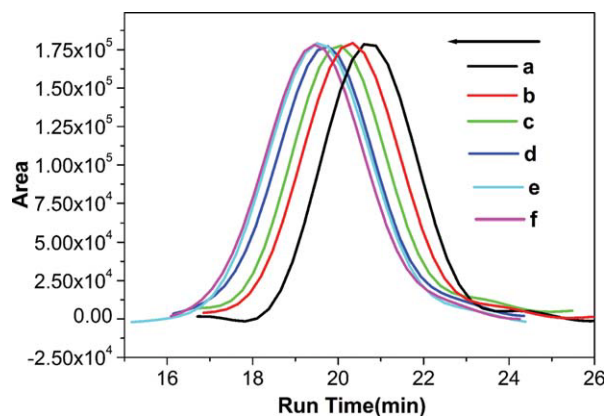


FIGURE 3 The GPC traces of the PFStODO. (a) $M_{n(\text{GPC})} = 10,000 \text{ g/mol}$, PDI = 1.20; (b) $M_{n(\text{GPC})} = 12,300 \text{ g/mol}$, PDI = 1.28; (c) $M_{n(\text{GPC})} = 13,900 \text{ g/mol}$, PDI = 1.26; (d) $M_{n(\text{GPC})} = 16,200 \text{ g/mol}$, PDI = 1.30; (e) $M_{n(\text{GPC})} = 17,100 \text{ g/mol}$, PDI = 1.32; (f) $M_{n(\text{GPC})} = 18,000 \text{ g/mol}$, PDI = 1.33.

polymerization is well controlled (Fig. 2). The $M_{n(\text{GPC})}$ s were lower than the correspondent $M_{n(\text{th})}$ s, in which the $M_{n(\text{th})}$ s was calculated according to $M_{n(\text{th})} = M_{w,4\text{Bri-Bu}} + ([\text{FStODO}]_0/[\text{4Bri-Bu}]_0) \times M_{w,\text{FStODO}} \times \text{Conversion}$ ($M_{w,4\text{Bri-Bu}}$ and $M_{w,\text{FStODO}}$ were the total molecular weight of 4Bri-Bu and FStODO and $[\text{FStODO}]_0$ and $[\text{4Bri-Bu}]_0$ means the initial concentrations of FStODO and 4Bri-Bu, respectively). The GPC chromatograms (Fig. 3) display narrow, single peaks and demonstrate that there are no low molecular weight

trails indicative of transfer processes. Therefore, the $M_{n(\text{GPC})}$ s deviated from the $M_{n(\text{th})}$ s that may be caused by the lower hydrodynamic volumes of star-branched polymers compared with their linear analogs.^{24–26}

Characterization of Star-Shaped Polymer

The star-shaped polymer was also characterized by ^1H NMR spectra and TG-DSC measurement. Figure 4 exhibits the ^1H NMR spectra of PFStODO, in which the signals of hydrogen

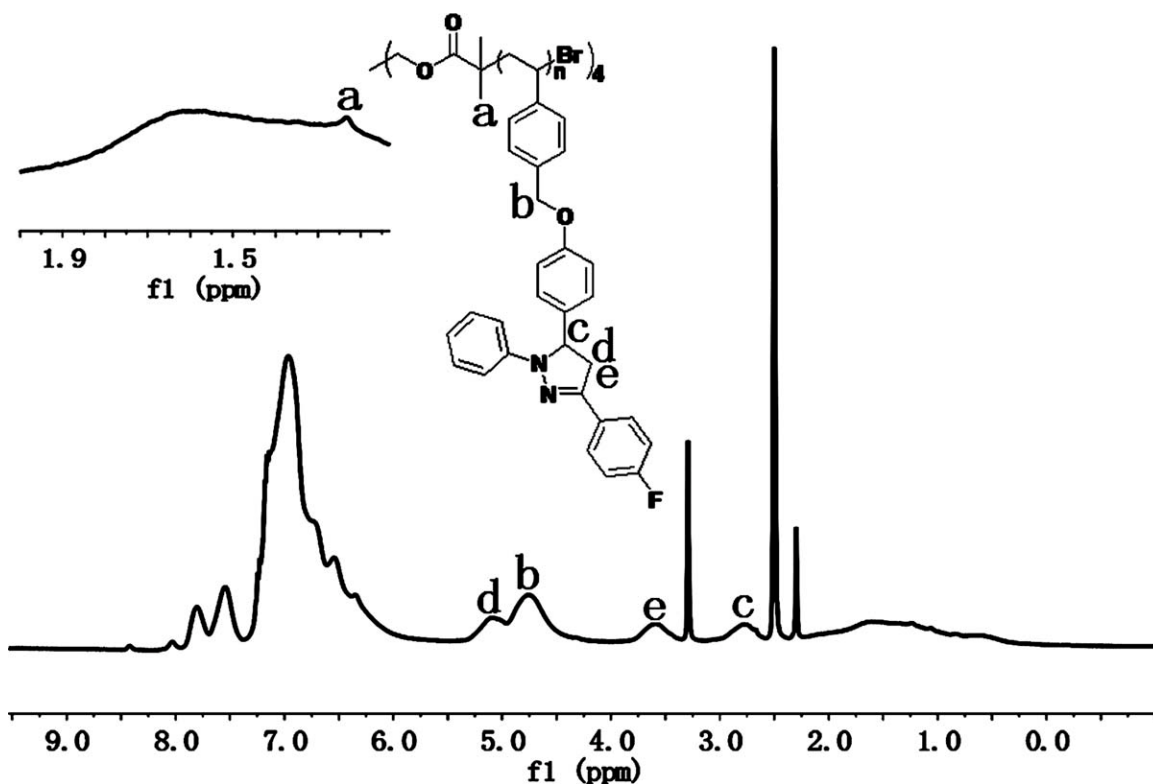


FIGURE 4 ^1H NMR spectrum in $\text{DMSO-}d_6$ of PFStODO ($M_{n(\text{GPC})} = 17,100 \text{ g/mol}$, PDI = 1.32).

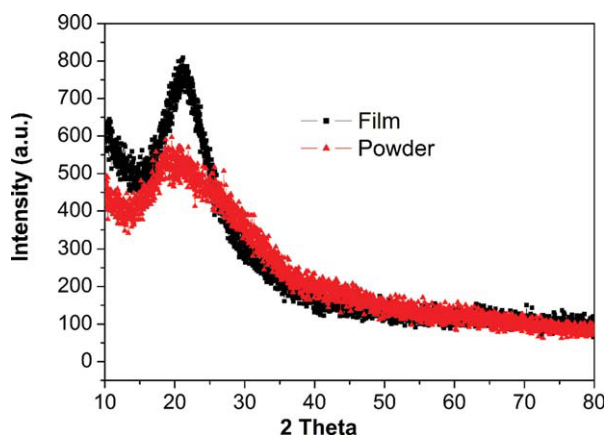


FIGURE 5 Powder and film XRD pattern of PFStODO.

atom from the vinyl group (5.5–6.0 ppm) were disappeared, and a broad signal of methylene below 2.0 ppm was formed. Furthermore, the signal of methyl groups adjacent to the bromine atoms in initiator at 1.91 ppm (Supporting Information) is disappeared in polymer, and new signal at 1.23 ppm may be assigned to those methyl groups and the chemical shift can be due to the longer distance of terminal bromine and methyl group. Hence, the ^1H NMR spectrum along with GPC results indicates the successful synthesis of star polymer.

The PFStODO also exhibits good thermal stability, with a glass transition temperature of about 145 °C and an onset decomposition temperature of about 290 °C, determined by differential scanning calorimetry and thermogravimetric analysis, respectively (Supporting Information).

XRD Analysis

XRD analysis was performed to clarify the aggregate of powder and film. According to Figure 5, the XRD results show that the powder has a broad diffraction peak at 19°, whereas that of film has a relatively sharp peak with a slightly red-shifted to 21°. It indicates that the bulk pyrazoline groups at the side chains were in more ordered aggregates in film.

Optical Properties in Organic Solution

All photophysical data of FStODO and its polymer are listed in Table 1. PFStODO exhibits good solubility in organic solvents such as CHCl_3 , THF, and DMF. As shown in Figure 6, absorption spectra of both monomer and its polymer in DMF solution are similar with $\lambda_{\text{max}} = 360$ nm, which can be assigned to the $\pi\text{-}\pi^*$ transition localized on the pyrazoline ring system.

The OPF in solution (5×10^{-5} mol/L) was first studied with λ_{ex} at 360 nm for FStODO and 340 nm for polymer (5×10^{-6} mol/L). The fluorescence of monomer and its polymer in DMF solution with different concentrations are also investigated (Figures were provided in Supporting Information). In all cases, the emission intensity reaches to a highest value (5×10^{-5} mol/L as to FStODO and 5×10^{-6} mol/L

TABLE 1 Photophysical Data for FStODO and PFStODO in Dilute DMF Solutions

Compounds	$\lambda_{\text{max}}^{\text{a}}$	$\lambda_{\text{max}}^{\text{b}}$	$\lambda_{\text{max}}^{\text{c}}$	$\lambda_{\text{max}}^{\text{d}}$	Φ^{e}	$\delta_{\text{max}}^{\text{f}}$
FStODO	360	460	730	462,482	0.73	13
PFStODO	360	460	730	462,482	0.40	203

^a The maximum wavelength of the UV–vis absorption spectra (nm).

^b The maximum wavelength of the fluorescence emission spectra (nm).

^c The maximum wavelength of the TPA spectra (nm).

^d The maximum wavelength of the two-photon fluorescence emission spectra (nm).

^e Fluorescence quantum yield.

^f Two photon cross section (GM).

as to PFStODO) with the concentration increasing at first and then decrease with continuous concentration increasing. As shown in Figure 6, the fluorescence intensity decreases from monomer to polymer with the number of the pyrazoline chromophore increasing. Accordingly, the fluorescence quantum yields [solution fluorescence quantum yield of the target compound was measured in DMF dilute solutions using quinine bisulfate ($\Phi_{\text{f}} = 0.546$ in 0.1 N H_2SO_4) as standards] of polymer (0.40) are obviously smaller than that of monomer (0.73), which can be attributed to the reabsorption of emitted photons^{11,12} and the self-quenching due to the intramolecular and intermolecular interactions of polymer.^{27–29} The fluorescence lifetime of FStODO and PFStODO in DMF solution were also studied as shown in Figure 7. There is biexponential decay, and the lifetime value of the monomer is observed to be longer than that of polymer. The result with the quantum yield may attribute to the electron transition of the monomer that is easier than that of the polymers.

TPEF spectra at the same concentration and the same pumped power under 720 nm excitation are depicted in Figure 8(a). The emission pattern of the monomer and polymer are similar but different with those in OPF. There is a comparable broad band with two maximum wavelengths of $\lambda_{\text{em1}} = 462$ nm and $\lambda_{\text{em2}} = 482$ nm in TPEF, whereas only one

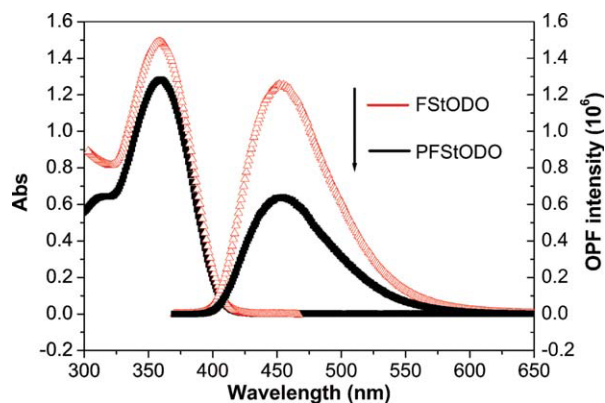


FIGURE 6 Linear absorption (left) and OPF (right) spectra of FStODO and PFStODO in DMF.

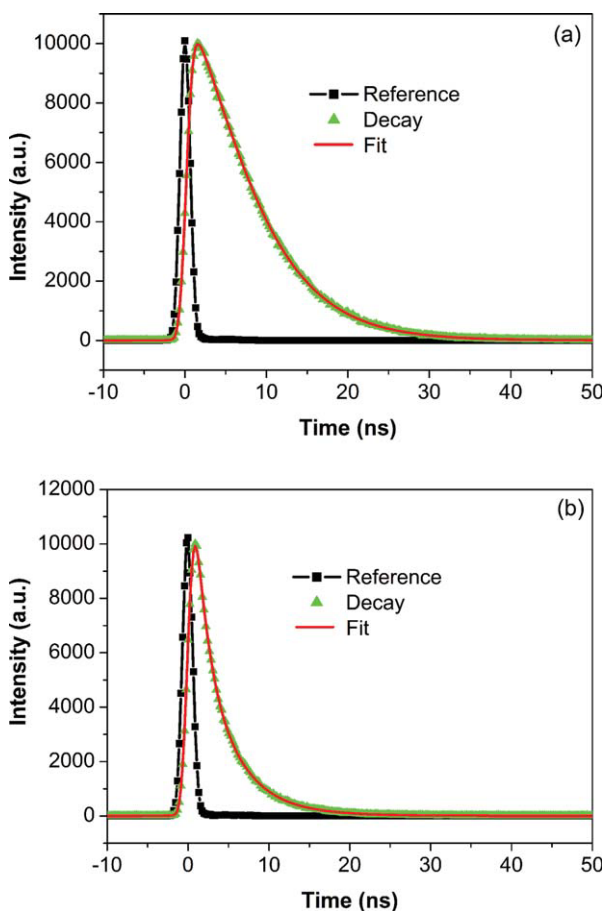


FIGURE 7 Typical fluorescence decay curves associated with lamp profile for the monomer (a) and its polymer (b) in ambient environment. Curve is shown in biexponential fits. Excitation wavelength is kept at 360 nm.

broad band with $\lambda_{em} = 460$ nm in OPF. Generally, most reported emission patterns of OPF and TPEF are similar. However, the chromophore aggregation or different excitation process will affect emission pattern. Herein, we temporarily attribute it to the molecule aggregation.

The inset figure of Figure 8(a) depicts the logarithmic plot of the TPEF integral versus the pumped power. The slope value obtained ($k = 1.82$ and 1.96), close to 2, indicates that TPA is the main excitation mechanism in the femtosecond regime.^{30,31}

The two-photon cross sections of the monomer and polymers in DMF at different excitation wavelengths are shown in Figure 8(b). The monomer and its polymer display a gradual increasing trend in TPA cross section with the maxima TPA cross-section value of 13 GM for FStODO and 203 GM for PFStODO. It is clear that the maxima TPA cross-section value increases with the number of pyrazoline chromophore. Obviously, the polymerization improves the TPA cross-section value.

Optical Properties at Film

Emission at a higher concentration (0.5 mmol/L) of polymer in DMF is measured. Except the band at 450 nm, a new band at 560 nm appeared in the emission pattern, indicating the excimer formation at high concentration (Supporting Information).³² Therefore, optical property of films of PFStODO is studied to confirm the excimer formation. The films of PFStODO are prepared by two methods: one is dipping the 1,2-dichloroethane (DCE) solution or THF solution (0.5 mmol/L) onto quartz surface, and the other is by spin coating using DCE solution. Figure 8 shows the absorption (left) and emission (right) pattern of PFStODO films. Compared to that of PFStODO solution, the main absorption band at 360 nm remains, but the new small absorption band at 460 nm appears ascribing to the aggregates of chromophore molecules.³³ More importantly, emission of films is quite different and appears as two main broad emission bands at 450 and 560 nm. It covers almost the whole visible-light spectrum (400–700 nm). The inner figure of Figure 8 is white

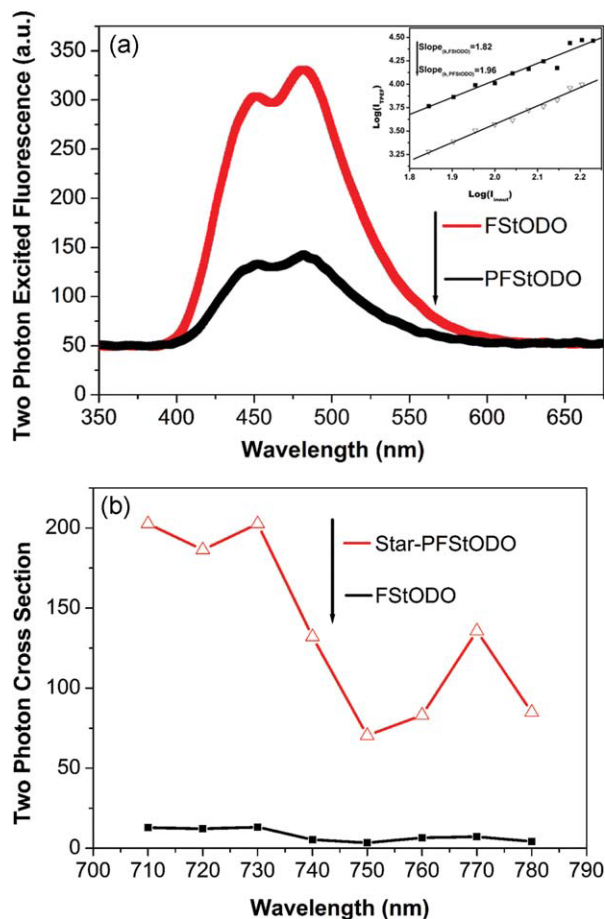


FIGURE 8 (a) TPF spectra of FStODO and PFStODO in DMF solution at 720 nm, inset is the dependence of output fluorescence intensity (I_{out}) of FStODO and PFStODO on the input laser power (I_{in}) at 720 nm in DMF solution. (b) TPA cross sections of FStODO and PFStODO in 710–780 nm regions.

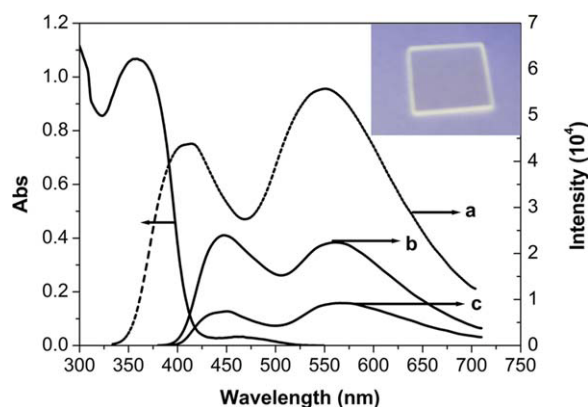


FIGURE 9 Linear absorption (left) and OPF (right) spectra of PFStODO at film state ($\lambda_{\text{ex}} = 360$ nm). (a) Spin-coating of DCE solution; (b) dipping of THF solution; and (c) dipping of DCE solution.

emission of transparent film under 365 nm UV light. The shorter band is assigned to emission of pyrazoline chromophore itself, whereas the longer band might be caused by formation of excimer in film.^{34–37} The quantum yield (QY) and fluorescent lifetime of film are also measured according to ref.³⁸; the QY of film is 1%, and the lifetime is 1.56 ns. The shorter lifetime confirm the formation of excimer. Compared with the XRD results, we considered that excimer formation is probably due to the ordered aggregates of pyrazoline chromophore at the side chains.

It is seldom reported that white-emission materials are obtained only by adjusting molecular aggregates (Fig. 9).

CONCLUSIONS

In summary, a novel blue fluorescent monomer with pyrazoline segment was synthesized, and its star-shaped polymer was obtained by ATRPs. The polymer emits strong blue fluorescence at 465 nm with the fluorescence quantum yields 0.40. Moreover, polymer shows obvious two-photon fluorescence with the cross-section value of 203 GM, much higher than that of monomer (13 GM). More interestingly, the film of PFStODO can emit white-light due to the excimer formation caused by the chromophore aggregates. Although the emission mechanism is still glancing, it might be a novel approach for designing new white emission materials tuned by molecule aggregates.

The authors gratefully thank Prof. Sun Baoquan for measurement of the quantum yield and life time of luminescence. The authors also thank Chinese Natural Science Foundation (Nos. 20876101, 200909044, and 21071105), major project of college and universities Jiangsu Province (08KJA430004), and a project funded by the Priority Academic Program Development of Jiangsu Higher Education Institutions.

REFERENCES AND NOTES

1 Shi, H. B.; Ji, S. J.; Bian, B. *Dyes Pigments* **2007**, *73*, 394–396.

- 2 Sano, T.; Nishio, Y.; Hamada, Y.; Takahashi, H.; Usuki, T.; Shibata, K. *J. Mater. Chem.* **2000**, *10*, 157–161.
- 3 Zhao, Y. S.; Fu, H. B.; Peng, A. D.; Ma, Y.; Liao, Q.; Yao, J. N. *Acc. Chem. Res.* **2010**, *43*, 409–418.
- 4 Barberá, J.; Clays, K.; Giménez, R.; Houbrechts, S.; Persoons, A.; Serrano, J. L. *J. Mater. Chem.* **1998**, *8*, 1725–1730.
- 5 Zhao, P. L.; Wang, F.; Zhang, M. Z.; Liu, Z. M.; Huang, W.; Yang, G. F. *J. Agric. Food Chem.* **2008**, *56*, 10767–10773.
- 6 Song, W. J.; Wang, Y. Z.; Yu, Z. P.; Vera, C. R.; Qu, J.; Lin, Q. *ACS Chem. Biol.* **2010**, *5*, 875–885.
- 7 Meyers, M. J.; Arhancet, G. B.; Hockerman, S. L.; Chen, X. Y.; Long, S. A.; Mahoney, M. W.; Rico, J. R.; Garland, D. J.; Blinn, J. R.; Collins, J. T.; Yang, S. T.; Huang, H.-C.; McGee, K. F.; Wendling, J. M.; Dietz, J. D.; Payne, M. A.; Homer, B. L.; Heron, M. I.; Reitz, D. B.; Hu, X. *J. Med. Chem.* **2010**, *53*, 5979–6002.
- 8 Palaska, E.; Erol, D.; Demirdamar, R. *Eur. J. Med. Chem.* **1996**, *31*, 43–47.
- 9 Banerjee, P.; Pramanik, S.; Sarkar, A.; Bhattacharya, S. C. *J. Phys. Chem. B* **2009**, *113*, 11429–11436.
- 10 Shen, F. G.; Peng, A. D.; Chen, Y.; Dong, Y.; Jiang, Z. W.; Wang, Y. B.; Fu, H. B.; Yao, J. N. *J. Phys. Chem. A* **2008**, *112*, 2206–2210.
- 11 Fahrni, C. J.; Yang, L. C.; VanDerveer, D. G. *J. Am. Chem. Soc.* **2003**, *125*, 3799–3812.
- 12 Cody, J.; Mandal, S.; Yang, L. C.; Fahrni, C. J. *J. Am. Chem. Soc.* **2008**, *130*, 13023–13032.
- 13 Armaroli, N.; Accorsi, G.; Gisselbrecht, J. P.; Hadziioannou, G.; Langa, F.; Nierengarten, J. F., et al. *J. Mater. Chem.* **2002**, *12*, 2077–2087.
- 14 Donohue, A. C.; Pallich, S.; McCarthy, T. D. *J. Chem. Soc., Perkin Trans. 1*, **2001**, 2817–2822.
- 15 Zhang, H. X.; Chen, H.; Li, Y.; Jiang, Q.; Xie, M. G. *Polym. Bull.* **2006**, *57*, 121–128.
- 16 Peng, Q.; Lu, Z. Y.; Huang, Y.; Xie, M. G.; Xiao, D.; Han, S. H.; Peng, J. B.; Cao, Y. *J. Mater. Chem.* **2004**, *14*, 396–401.
- 17 Chen, H.; Xu, X.; Yan, H. G.; Cai, X. R.; Li, Y.; Jiang, Q.; Xie, M. G. *Chin. Chem. Lett.* **2007**, *18*, 1496–1500.
- 18 Qi, Y.; Li, N. J.; Xia, X. W.; Ge, J. F.; Lu, J. M.; Xu, Q. F. *Mater. Chem. Phys.* **2010**, *124*, 726–731.
- 19 Gao, H. F.; Matyjaszewski, K. *Prog. Polym. Sci.* **2009**, *34*, 317–350.
- 20 Zhang, L.; Xu, Q. F.; Lu, J. M.; Li, N. J.; Yan, F.; Wang, L. H. *Polymer* **2009**, *50*, 4807–4812.
- 21 Lu, J. M.; Xu, Q. F.; Yuan, X.; Xia, X. W.; Wang, L. H. *J. Polym. Sci. Part A: Polym. Chem.* **2009**, *47*, 4800–4901.
- 22 Wang, G. W.; Luo, X. L.; Zhang, Y. N.; Huang, J. L. *J. Polym. Sci. Part A: Polym. Chem.* **2007**, *45*, 3894–4810.
- 23 Xu, C.; Webb, W. W. *J. Opt. Soc. Am. B* **1996**, *13*, 481–491.
- 24 Matyjaszewski, K.; Miller, P. J.; Pyun, J.; Kickelbick, G.; Diamanti, S. *Macromolecules* **1999**, *32*, 6526–6535.
- 25 Ueda, J.; Kamigaito, M.; Sawamoto, M. *Macromolecules* **1998**, *31*, 6762–6768.
- 26 Angot, S.; Murthy, S.; Taton, D.; Gnanou, Y. *Macromolecules* **1998**, *31*, 7218–7225.
- 27 Jagadeesh, B.; Bodapati, Huriye, Icil. *Dyes Pigments* **2008**, *79*, 224–235.
- 28 Ding, L. P.; Dominska, M.; Fang, Y.; Blanchard, G. J. *Electrochim. Acta* **2008**, *53*, 6704–6713.
- 29 Yan, Y. X.; Fan, H. H.; Lam, C. K.; Huang, H.; Wang, J.; Hu, S.; Wang, H. Z.; Chen, X. M. *Bull. Chem. Soc. Jpn.* **2006**, *79*, 1614–1619.

- 30** Zhao, Y. X.; Li, X.; Wu, F. P.; Fang, X. Y. *J. Photochem. Photobiol. A* **2006**, *177*, 12–16.
- 31** Wang, X. M.; Jin, F.; Chen, Z. G.; Liu, S. Q.; Wang, X. H.; Duan, X. M.; Tao, X. T.; Jiang, M. H. *J. Phys. Chem. C* **2011**, *115*, 776–784.
- 32** Winnik, F. M. *Chem. Rev.* **1993**, *93*, 587–614.
- 33** Su, L. H.; Bao, C. Y.; Lu, R.; Chen, Y. L.; Xu, T. H.; Song, D. P.; Tan, C. H.; Shi, T. S.; Zhao, Y. Y. *Org. Biomol. Chem.* **2006**, *4*, 2591–2594.
- 34** Liao, L.; Pang, Y. *Macromolecules* **2001**, *34*, 7300–7305.
- 35** Huang, B.; Li, J.; Jiang, Z. Q.; Qin, J. G.; Yu, G.; Liu, Y. Q. *Macromolecules* **2005**, *38*, 6915–6922.
- 36** Laughlin, B. J.; Smith, R. C. *Macromolecules* **2010**, *43*, 3744–3749.
- 37** Shi, Q. Q.; Chen, W. Q.; Xiang, J. F.; Duan, X. M.; Zhan, X. W. *Macromolecules* **2011**, *44*, 3759–3765.
- 38** Lakowicz, J. R. *Principles of Fluorescence Spectroscopy*; Springer: Singapore, **2006**; Chapter 2, pp 54–55; Chapter 4, p 98.